DFG Deutsche Forschungsgemeinschaft
Priority Programme 1962

Strong vs. Weak Symmetry in Stress-based Mixed Finite Element Methods for Linear Elasticity

Bernhard Kober, Gerhard Starke

SPP 1962 | Non-smooth and Complementarity-based Distributed Parameter Systems: Simulation and Hierarchical Optimization

Preprint Number SPP1962-104

received on February 25, 2019

Edited by
SPP1962 at Weierstrass Institute for Applied Analysis and Stochastics (WIAS)
Leibniz Institute in the Forschungsverbund Berlin e.V.
Mohrenstraße 39, 10117 Berlin, Germany
E-Mail: spp1962@wias-berlin.de

World Wide Web: http://spp1962.wias-berlin.de/

Strong vs. Weak Symmetry in Stress-Based Mixed Finite Element Methods for Linear Elasticity

Bernhard Kober and Gerhard Starke

Fakultät für Mathematik, Universität Duisburg-Essen, Thea-Leymann-Str. 9, 45127 Essen, Germany {bernhard.kober,gerhard.starke}@uni-due.de

Abstract. Based on the Hellinger-Reissner principle, accurate stress approximations can be computed directly in suitable $H(\mathrm{div})$-like finite element spaces treating conservation of momentum and the symmetry of the stress tensor as constraints. Two stress finite element spaces of polynomial degree 2 which were proposed in this context will be compared and relations between the two will be established. The first approach uses Raviart-Thomas spaces of next-to-lowest degree and is therefore $H(\mathrm{div})$-conforming but produces only weakly symmetric stresses. The stresses obtained from the second approach satisfy symmetry exactly but are nonconforming with respect to $H(\mathrm{div})$. It is shown how the latter finite element space can be derived by augmenting the componentwise next-to-lowest Raviart-Thomas space with suitable bubbles. However, the convergence order of the resulting stress approximation is reduced from two to one as will be confirmed by numerical results. Finally, the weak stress symmetry property of the first approach is discussed in more detail and a post-processing procedure for the construction of stresses which are element-wise symmetric on average is proposed.

1 Introduction

The Hellinger-Reissner principle formulates the variational problem of linear elasticity in terms of stresses alone with conservation of momentum and stress symmetry as constraints. A number of finite element combinations were proposed for this approach starting with [1], see [2] and [4] for a recent overview of the state-of-the-art. Two particularly appealing stress finite elements which are of lowest possible (to achieve quadratic convergence) polynomial degree 2 are investigated in this contribution. The first one is due to Boffi, Brezzi and Fortin [3] and uses Raviart-Thomas spaces of next-to-lowest degree for the stress approximation which is only weakly symmetric. The second one is due to Gopalakrishnan and Guzmán [7] and produces exactly symmetric stresses but is nonconforming with respect to $H(\mathrm{div})$. In contrast to the derivation in [7] where symmetric basis functions for the stress approximation are used, we will enforce (exact) symmetry by Lagrange multipliers here. To this end, a nonsymmetric version of their nonconforming stress space is introduced and shown to be obtained from augmenting the componentwise next-to-lowest order Raviart-Thomas space with suitable bubbles (four per element in the two-dimensional case).

2 The Hellinger-Reissner Principle and Stress Finite Element Spaces

We consider the reference configuration $\Omega \subset \mathbb{R}^d$ ($d = 2, 3$) of a linear elastic object with boundary $\partial\Omega = \Gamma = \overline{\Gamma_N} \cup \overline{\Gamma_D}$ (Γ_N and Γ_D disjoint and nonempty), a volume load $\mathbf{f} : \Omega \mapsto \mathbb{R}^d$ and some prescribed displacement $\mathbf{u}_D : \Gamma_D \mapsto \mathbb{R}^d$ and surface forces $\mathbf{g} : \Gamma_N \mapsto \mathbb{R}^d$ on the separate boundary parts. The Hellinger-Reissner Principle can then be obtained by considering the optimality conditions for minimizing the elastic energy in terms of stress

$$\mathcal{J}(\boldsymbol{\sigma}) := \frac{1}{2}\int_\Omega (\mathcal{A}\boldsymbol{\sigma}) : \boldsymbol{\sigma}\, dx - \int_{\Gamma_D} (\boldsymbol{\sigma}\cdot\mathbf{n})\cdot\mathbf{u}_D\, ds$$

constrained by $\operatorname{div}\boldsymbol{\sigma} = -\mathbf{f}$, $\mathbf{as}\,\boldsymbol{\sigma} = \mathbf{0}$ in Ω and $\boldsymbol{\sigma}\cdot\mathbf{n} = \mathbf{g}$ on Γ_N.

Here $\boldsymbol{\sigma} : \Omega \mapsto \mathbb{R}^{dxd}$ denotes the stress tensor, $\mathbf{n}$ denotes the outer unit normal, $\mathbf{as}$ denotes the antisymmetric part of a matrix, div denotes the divergence (applied row-wise) and $\mathcal{A}$ denotes the compliance tensor given by

$$\mathcal{A}\boldsymbol{\sigma} := \frac{1}{2\mu}\left(\boldsymbol{\sigma} - \frac{\lambda}{d\lambda + 2\mu}(\operatorname{tr}\boldsymbol{\sigma})\mathbf{I}\right) \tag{1}$$

with the material dependent Lamé constants λ and μ. In the incompressible limit ($\lambda \to \infty$) $\mathcal{A}\boldsymbol{\sigma}$ is reduced to the deviatoric (trace-free) part of $\boldsymbol{\sigma}$ (and thus remains bounded). The problem is then to find $\boldsymbol{\sigma} \in \boldsymbol{\Sigma}$ with $\boldsymbol{\sigma}\cdot\mathbf{n} = \mathbf{g}$ on Γ_N, $\mathbf{u} \in \boldsymbol{U}$ and $\boldsymbol{\theta} \in \boldsymbol{\Theta}$ satisfying

$$\begin{aligned} (\mathcal{A}\boldsymbol{\sigma}, \boldsymbol{\tau})_0 + (\mathbf{u}, \operatorname{div}\boldsymbol{\tau})_0 + (\boldsymbol{\theta}, \mathbf{as}\,\boldsymbol{\tau})_0 &= (\mathbf{u}_D, \boldsymbol{\tau}\cdot\mathbf{n})_{0,\Gamma_D}\ , \\ (\operatorname{div}\boldsymbol{\sigma}, \mathbf{v})_0 &= -(\mathbf{f}, \mathbf{v})_0\ , \\ (\mathbf{as}\,\boldsymbol{\sigma}, \boldsymbol{\gamma})_0 &= 0\,, \end{aligned} \tag{2}$$

for all $\boldsymbol{\tau} \in \boldsymbol{\Sigma}$ with $\boldsymbol{\tau}\cdot\mathbf{n} = \mathbf{0}$ on Γ_N, $\mathbf{v} \in \boldsymbol{U}$ and $\boldsymbol{\gamma} \in \boldsymbol{\Theta}$. Here, $(\cdot,\cdot)_0$ and $(\cdot,\cdot)_{0,\Gamma_D}$ denote the L^2 inner products on Ω and Γ_D.

The used function spaces are defined as follows

$$\begin{aligned} \boldsymbol{\Sigma} &:= H(\Omega, \operatorname{div})^d = \{\boldsymbol{\tau} \in L^2(\Omega)^d : \operatorname{div}\mathbf{v} \in L^2(\Omega)\}^d, \\ \boldsymbol{U} &:= L^2(\Omega)^d, \\ \boldsymbol{\Theta} &:= L^2(\Omega)^{d\times d,\mathbf{as}} = \{\boldsymbol{\gamma} \in L^2(\Omega)^{d\times d} : \boldsymbol{\gamma} + \boldsymbol{\gamma}^{\mathrm{T}} = \mathbf{0}\}, \end{aligned}$$

where the Lagrange multiplier enforcing the divergence constraint can be interpreted as the displacement and the one enforcing the symmetry constraint as the antisymmetric part of the gradient of displacement, i.e. the rotations. The saddle point problem (2) is wellposed (see [3]).

Using finite dimensional (sub)spaces one obtains the corresponding mixed finite element method:

Find $\boldsymbol{\sigma}_h \in \boldsymbol{\Sigma}_h$ with $\boldsymbol{\sigma}_h \cdot \mathbf{n} = \mathbf{g}$ on Γ_N, $\mathbf{u}_h \in \boldsymbol{U}_h$ and $\boldsymbol{\theta}_h \in \boldsymbol{\Theta}_h$ satisfying

$$\begin{aligned}(\mathcal{A}\boldsymbol{\sigma}_h, \boldsymbol{\tau}_h)_0 + (\mathbf{u}_h, \operatorname{div} \boldsymbol{\tau}_h)_0 + (\boldsymbol{\theta}_h, \mathbf{as}\, \boldsymbol{\tau}_h)_0 &= (\mathbf{u}_D, \boldsymbol{\tau}_h \cdot \mathbf{n})_{0,\Gamma_D}\,, \\ (\operatorname{div} \boldsymbol{\sigma}_h, \mathbf{v}_h)_0 &= -(\mathbf{f}, \mathbf{v}_h)_0\,, \\ (\mathbf{as}\, \boldsymbol{\sigma}_h, \boldsymbol{\gamma}_h)_0 &= 0,\end{aligned} \tag{3}$$

for all $\boldsymbol{\tau}_h \in \boldsymbol{\Sigma}_h$ with $\boldsymbol{\tau}_h \cdot \mathbf{n} = \mathbf{0}$ on Γ_N, $\mathbf{v}_h \in \boldsymbol{U}_h$ and $\boldsymbol{\gamma}_h \in \boldsymbol{\Theta}_h$.

For the work with finite element spaces we denote by $\mathcal{T}_h$ a simplicial mesh of Ω with the set of sides $\mathcal{S}_h$ and by $\mathcal{P}_k(T)$ the polynomials of degree k or less on a simplex $T \in \mathcal{T}_h$. The first finite element combination which we consider was suggested in [3] and features next-to-lowest degree Raviart-Thomas elements:

$$\begin{aligned}\mathcal{RT}_k(T) &:= \{\mathbf{p}(\mathbf{x}) + \mathbf{x}\tilde{p}(\mathbf{x}) : \mathbf{p} \in \mathcal{P}_k(T)^d,\, \tilde{p} \in \mathcal{P}_k(T)\} \\ \boldsymbol{\Sigma}_h &:= \mathcal{RT}_1(\mathcal{T}_h)^d = \{\boldsymbol{\tau}_h \in \boldsymbol{\Sigma} : \boldsymbol{\tau}_h|_T \in \mathcal{RT}_1(T)^d \;\forall\, T \in \mathcal{T}_h\} \\ \boldsymbol{U}_h &:= \mathcal{DP}_1(\mathcal{T}_h)^d = \{\mathbf{v}_h \in \boldsymbol{U} : \mathbf{v}_h|_T \in \mathcal{P}_1(T)^d \;\forall\, T \in \mathcal{T}_h\} \\ \boldsymbol{\Theta}_h &:= \mathcal{P}_1(\mathcal{T}_h)^{d\times d,\mathbf{as}} = \{\boldsymbol{\gamma}_h \in \boldsymbol{\Theta} \cap C(\Omega)^{d\times d} : \boldsymbol{\gamma}_h|_T \in \mathcal{P}_1(T)^{d\times d} \;\forall\, T \in \mathcal{T}_h\}\end{aligned}$$

The second combination as suggested in [7] uses strongly symmetric stress approximations and thus the second Lagrange multiplier is no longer needed. $\boldsymbol{U}_h$ remains the same but $\boldsymbol{\Sigma}_h$ is replaced by:

$$\begin{aligned}\boldsymbol{\Sigma}_h^{\mathrm{S}} := \{&\boldsymbol{\tau}_h \in L^2(\Omega)^{2\times 2} : \mathbf{as}\, \boldsymbol{\tau}_h = \mathbf{0},\, \boldsymbol{\tau}_h|_T \in \mathcal{P}_2(T)^{2\times 2} \text{ for all } T \in \mathcal{T}_h, \\ &(\llbracket \boldsymbol{\tau}_h \cdot \mathbf{n}_S \rrbracket_S, \mathbf{p}_1)_{0,S} = 0 \text{ for all } \mathbf{p}_1 \in \mathcal{P}_1(S)^2 \text{ for all } S \in \mathcal{S}_h\}.\end{aligned} \tag{4}$$

Where $\llbracket \cdot \rrbracket_S$ denotes the jump over the side S. Since $\boldsymbol{\Sigma}_h^{\mathrm{S}} \not\subset \boldsymbol{\Sigma}$, this combination yields a non-conforming method and requires the use of an element-wise divergence operator div_h. The problem is then to find $\boldsymbol{\sigma}_h \in \boldsymbol{\Sigma}_h^{\mathrm{S}}$ with $(\llbracket \boldsymbol{\sigma}_h \cdot \mathbf{n}_S - \mathbf{g} \rrbracket_S, \mathbf{p}_1)_{0,S} = 0$ for $S \subset \Gamma_N$ and $\mathbf{u}_h \in \boldsymbol{U}_h$ satisfying

$$\begin{aligned}(\mathcal{A}\boldsymbol{\sigma}_h, \boldsymbol{\tau}_h)_0 + (\mathbf{u}_h, \operatorname{div}_h \boldsymbol{\tau}_h)_0 &= (\mathbf{u}_D, \boldsymbol{\tau}_h \cdot \mathbf{n})_{0,\Gamma_D}\,, \\ (\operatorname{div}_h \boldsymbol{\sigma}_h, \mathbf{v}_h)_0 &= -(\mathbf{f}, \mathbf{v}_h)_0\end{aligned} \tag{5}$$

for all $\boldsymbol{\tau}_h \in \boldsymbol{\Sigma}_h^{\mathrm{S}}$ with $(\boldsymbol{\tau}_h \cdot \mathbf{n}_S, \mathbf{p}_1)_{0,S} = 0$ for $S \subset \Gamma_N$ and $\mathbf{v}_h \in \boldsymbol{U}_h$.

Both methods are proven to be wellposed and convergent. For the first one standard results are used after verifying an inf-sup condition of the form

$$\inf_{\substack{\mathbf{v}_h \in \boldsymbol{U}_h \\ \boldsymbol{\gamma}_h \in \boldsymbol{\Theta}_h}} \sup_{\boldsymbol{\tau}_h \in \boldsymbol{\Sigma}_h} \frac{(\operatorname{div} \boldsymbol{\tau}_h, \mathbf{v}_h)_0 + (\mathbf{as}\, \boldsymbol{\tau}_h, \boldsymbol{\gamma}_h)_0}{\|\boldsymbol{\tau}_h\|_{\boldsymbol{\Sigma}}(\|\mathbf{v}_h\|_{\boldsymbol{U}} + \|\boldsymbol{\gamma}_h\|_{\boldsymbol{\Theta}})} \geq \beta, \tag{6}$$

and for the second one a direct analysis of the resulting linear system is necessary since the standard techniques are not applicable due to the non-conformity. Both stress spaces have good approximation properties but the non-conformity in the second method only allows an a-priori error estimate of order $\mathcal{O}(h)$, while the first one retains the optimal convergence order $\mathcal{O}(h^2)$.

3 The $H(\mathrm{div})$-nonconforming space by augmenting Raviart-Thomas Elements

Our aim is now to describe a method which uses Lagrange multipliers to find a solution in $\boldsymbol{\Sigma}_h^{\mathbb{S}}$, without having to construct symmetric basis functions. We therefore remove the symmetry requirement from our ansatz space:

$$\begin{aligned}\boldsymbol{\Sigma}_h^{\cup} := \{&\boldsymbol{\tau}_h \in L^2(\Omega)^{d\times d} : \boldsymbol{\tau}_h|_T \in \mathcal{P}_2(T)^{d\times d} \text{ for all } T \in \mathcal{T}_h,\\ &(\llbracket \boldsymbol{\tau}_h \cdot \mathbf{n}_S \rrbracket_S, \mathbf{p}_1)_{0,S} = 0 \text{ for all } \mathbf{p}_1 \in \mathcal{P}_1(S)^d \text{ for all } S \in \mathcal{S}_h\}.\end{aligned}$$

Moreover we extend the space of rotations to $\boldsymbol{\Theta}_h^{\cup} := \mathcal{DP}_2(\mathcal{T}_h)^{d\times d,\mathbf{as}}$ and propose the following:

Theorem 1. *The mapping* $\mathbf{as} : \boldsymbol{\Sigma}_h^{\cup} \to \boldsymbol{\Theta}_h^{\cup}$ *is surjective.*

We will give the idea of the proof after having a closer look at $\boldsymbol{\Sigma}_h^{\cup}$ in the next subsection, but first we want to state the following corollary.

Theorem 2. *If (5) has a unique solution, then the following problem has a unique solution and the stress and displacement approximations coincide: Find* $\boldsymbol{\sigma}_h \in \boldsymbol{\Sigma}_h^{\cup}$ *with* $(\llbracket \boldsymbol{\sigma}_h \cdot \mathbf{n}_S - \mathbf{g} \rrbracket_S, \mathbf{p}_1)_{0,S} = 0$ *for* $S \subset \Gamma_N$, $\mathbf{u}_h \in \boldsymbol{U}_h$ *and* $\boldsymbol{\theta}_h \in \boldsymbol{\Theta}_h^{\cup}$ *satisfying*

$$\begin{aligned}(\mathcal{A}\boldsymbol{\sigma}_h, \boldsymbol{\tau}_h)_0 + (\mathbf{u}_h, \operatorname{div}_h \boldsymbol{\tau}_h)_0 + (\boldsymbol{\theta}_h, \mathbf{as}\, \boldsymbol{\tau}_h)_0 &= (\mathbf{u}_D, \boldsymbol{\tau}_h \cdot \mathbf{n})_{0,\Gamma_D},\\ (\operatorname{div}_h \boldsymbol{\sigma}_h, \mathbf{v}_h)_0 &= -(\mathbf{f}, \mathbf{v}_h)_0,\\ (\mathbf{as}\, \boldsymbol{\sigma}_h, \boldsymbol{\gamma}_h)_0 &= 0,\end{aligned} \tag{7}$$

for all $\boldsymbol{\tau}_h \in \boldsymbol{\Sigma}_h^{\cup}$ *with* $(\boldsymbol{\tau}_h \cdot \mathbf{n}_S, \mathbf{p}_1)_{0,S} = 0$ *for* $S \subset \Gamma_N$, $\mathbf{v}_h \in \boldsymbol{U}_h$ *and* $\boldsymbol{\gamma}_h \in \boldsymbol{\Theta}_h$.

Proof. Suppose $(\boldsymbol{\sigma}_h, \mathbf{u}_h, \boldsymbol{\theta}_h)$ is solution of (7), then $\boldsymbol{\sigma}_h \in \boldsymbol{\Sigma}_h^S$ because of $\mathbf{as}\, \boldsymbol{\sigma}_h \in \boldsymbol{\Theta}_h^{\cup}$. Testing with $\boldsymbol{\tau}_h \in \boldsymbol{\Sigma}_h^S \subset \boldsymbol{\Sigma}_h^{\cup}$ immediately gives that $(\boldsymbol{\sigma}_h, \mathbf{u}_h)$ is also solution of (5). We now argue that, assuming the wellposedness of (5), the problem (7) with homogeneous right hand side $(\mathbf{f}, \mathbf{g}, \mathbf{u}_D = \mathbf{0})$ possesses only the zero solution. This is due to Theorem 1. The result then follows because (7) is a square system. □

Just like $\boldsymbol{\Theta}_h^{\cup}$ could be interpreted (locally) as an extension of $\boldsymbol{\Theta}_h$, the nonconforming space $\boldsymbol{\Sigma}_h^{\cup}$ can be described as an enrichment of $\boldsymbol{\Sigma}_h$ by an augmenting space $\boldsymbol{\Sigma}_h^{\Delta}$ consisting curls of certain bubble functions on each simplex.

3.1 The augmenting space $\boldsymbol{\Sigma}_h^{\Delta}$

The structure of $\boldsymbol{\Sigma}_h^{\Delta}$ is very similar for $d = 2$ and $d = 3$, so for lack of space we will describe it in two dimensions only. We will denote by λ_i^T, $i = 1, 2, 3$ the barycentric coordinates on the triangle T and by $\nabla^{\perp} := \begin{pmatrix}\partial_2 & -\partial_1\end{pmatrix}^{\mathrm{T}}$ the

orthogonal gradient (or 2D-curl). First we need to define the needed bubble functions.

For each triangle $T \in \mathcal{T}_h$ let $b_T(\mathbf{x}) := \lambda_1^T(\mathbf{x})\lambda_2^T(\mathbf{x})\lambda_3^T(\mathbf{x})$ (extended by zero outside T) be the cubic element-bubble-function on T and for each edge $S_i \in \partial T$ let $b_{T,S_i}(\mathbf{x}) := \lambda_i^T(\mathbf{x})\lambda_{i+1}^T(\mathbf{x})(\lambda_i^T(\mathbf{x}) - \lambda_{i+1}^T(\mathbf{x}))$ (extended by zero outside T) be the cubic edge-bubble-function of S_i on T. Note that while b_T vanishes on ∂T and thus is globally continuous, b_{T,S_i} vanishes only on S_j with $j \neq i$ and thus is not globally continuous.

Taking the curls of these functions we obtain the desired extension. We introduce the space of bubble-curls by

$$\mathcal{BC}(\mathcal{T}_h) := \operatorname{span}\{\nabla^\perp b_T, \nabla^\perp b_{T,S_1}, \nabla^\perp b_{T,S_2}, \nabla^\perp b_{T,S_3}\}_{T\in\mathcal{T}_h},$$

where $\nabla^\perp$ is to be understood elementwise. Finally the augmenting space is defined as

$$\boldsymbol{\Sigma}_h^\Delta := \mathcal{BC}(\mathcal{T}_h)^2$$

and we can obtain the following relationship:

Theorem 3.

$$\boldsymbol{\Sigma}_h^\cup = \boldsymbol{\Sigma}_h \oplus \boldsymbol{\Sigma}_h^\Delta$$

Proof. $\underline{\boldsymbol{\Sigma}_h \oplus \boldsymbol{\Sigma}_h^\Delta \subset \boldsymbol{\Sigma}_h^\cup}$: $\boldsymbol{\Sigma}_h \subset \boldsymbol{\Sigma}_h^\cup$ is trivial since $[\![\boldsymbol{\tau}_h \cdot \mathbf{n}_S]\!]_S = \mathbf{0}$ for $\boldsymbol{\tau}_h \in \boldsymbol{\Sigma}$. For $\boldsymbol{\tau}_h \in \boldsymbol{\Sigma}_h^\Delta$ we have to verify the jump condition

$$([\![\boldsymbol{\tau}_h \cdot \mathbf{n}_S]\!]_S, \mathbf{p}_1)_{0,S} = 0 \quad \forall\, \mathbf{p}_1 \in \mathcal{P}_1(S)^2,\ \forall\, S \in \mathcal{S}_h.$$

The simple identity $\mathbf{n}_S \cdot \nabla^\perp = \mathbf{t}_S \cdot \nabla$ suggests that we are to consider the tangential derivatives of the bubble functions. Those derivatives vanish on all edges except for one edge for each edge-bubble-function. However for the curl of an edge-bubble-function restricted to the nonzero edge we have

$$\begin{aligned}\mathbf{n}_{S_i} \cdot \nabla^\perp b_{T,S_i} &= \mathbf{t}_{S_i} \cdot \nabla(\lambda_i\lambda_{i+1}(\lambda_i - \lambda_{i+1})) \\ &= (\lambda_{i+1}(\lambda_i - \lambda_{i+1}) - \lambda_i(\lambda_i - \lambda_{i+1}) + 2\lambda_i\lambda_{i+1})(\mathbf{t}_{S_i} \cdot \nabla\lambda_i) \\ &= (-6\lambda_i^2 + 6\lambda_i - 1)(\mathbf{t}_{S_i} \cdot \nabla\lambda_i),\end{aligned}$$

which is zero when tested against linear functions on S_i.

$\underline{\boldsymbol{\Sigma}_h^\cup \subset \boldsymbol{\Sigma}_h \oplus \boldsymbol{\Sigma}_h^\Delta}$: On a single triangle we have $\dim \mathcal{RT}_1(T) = 8$ and $\dim \mathcal{BC}(T) = 4$. Since $\nabla^\perp b_T$ is zero at the center of mass of T and has vanishing normal component on ∂T we have $\nabla^\perp b_T \notin \mathcal{RT}_1(T)$. The same holds true for each $\nabla^\perp b_{T,S_i}$ since its normal component is a quadratic function on S_i. Therefore $\dim \mathcal{RT}_1(T) \oplus \mathcal{BC}(T) = 12 = \dim \mathcal{P}_2(T)^2$. □

Using this representation of $\boldsymbol{\Sigma}_h^\cup$ one can now prove Theorem 1 by combining a smart choice of basis functions of $\mathcal{RT}_1(\mathcal{T}_h)$ and $\mathcal{BC}(\mathcal{T}_h)$ to obtain a basis of $\boldsymbol{\Theta}_h^\cup$. Due to lack of space we will omit the details here and proceed with the presentation of our numerical results.

4 A Numerical Comparison

We tested both methods featuring Lagrange multipliers against the Cook's membrane problem, as well as against a regularized problem, both for a nearly incompressible ($\lambda = 49999$) and a compressible material ($\lambda = 2$). μ is always set to 1. The shape of Ω as well as the boundary conditions are summarized in figure 1 with $\mathbf{F}_c = \begin{pmatrix} 0 & 0.0625 \end{pmatrix}^{\mathrm{T}}$ and $\mathbf{F}(x_2) = 4\mathbf{F}_c \max\{0, 1 - 25|x_2 - 0.52|\}$. The volume load $\mathbf{f}$ was set to zero in both cases.

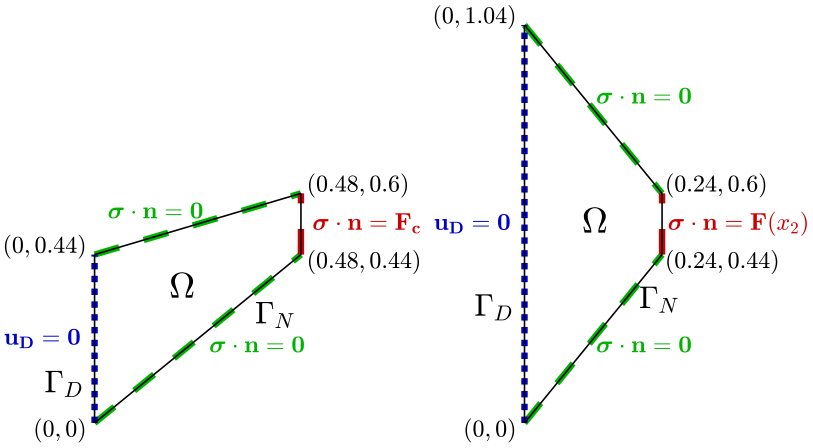

Fig. 1. cooks membrane on the left and the regularized domain on the right

Due to the lack of an analytical solution we need an alternative for assessing the quality of our approximations. The least-squares-functional

$$\mathcal{J}_{ls}(\boldsymbol{\sigma}_h, \mathbf{u}_h^R) := \frac{1}{2}\|\mathcal{A}\boldsymbol{\sigma}_h^{\$} - \boldsymbol{\varepsilon}(\mathbf{u}_h^R)\|_0^2 + \frac{1}{2}\|\mathbf{as}\,\boldsymbol{\sigma}_h\|_0^2,$$

with $\boldsymbol{\sigma}_h^{\$} := \boldsymbol{\sigma}_h - \mathbf{as}\,\boldsymbol{\sigma}_h$ and $\boldsymbol{\varepsilon}(\mathbf{u}_h^R) := \nabla\mathbf{u}_h^R - \mathbf{as}\,\nabla\mathbf{u}_h^R$ is equivalent to the approximation error (see [5, Theorem 3.1]). The displacement reconstruction $\mathbf{u}_h^R \in H^1(\Omega)$ necessary for the evalutation of $\mathcal{J}_{ls}(\boldsymbol{\sigma}_h, \mathbf{u}_h^R)$ is constructed following ideas from [6] and [8]: $\mathbf{u}_h^R$ is obtained by first solving the following problem locally on every triangle $T \in \mathcal{T}_h$:

$$\begin{aligned} \left(\boldsymbol{\nabla}\tilde{\mathbf{u}}_h^R, \boldsymbol{\nabla}\mathbf{v}_h\right)_0 + (\mathbf{p}_h, \mathbf{v}_h)_0 &= (\mathcal{A}\boldsymbol{\sigma}_h + \boldsymbol{\theta}_h, \boldsymbol{\nabla}\mathbf{v}_h)_0 \qquad && \forall\, \mathbf{v}_h \in \mathcal{P}_2(T)^2, \\ \left(\tilde{\mathbf{u}}_h^R, \mathbf{q}_h\right)_0 &= (\mathbf{u}_h, \mathbf{q}_h)_0 && \forall\, \mathbf{q}_h \in \mathcal{P}_0(T)^2 \end{aligned} \tag{8}$$

and subsequently averaging the values of $\tilde{\mathbf{u}}_h^R$ on the vertices and edge midpoints to retrieve $\mathbf{u}_h^R \in \mathcal{P}_2(\mathcal{T}_h)^2 \subset H^1(\Omega)$.

The results for the Cook's membrane problem are summarized in table 1, where $l := \log_2(h_0/h)$ is the level of refinement, $\boldsymbol{\sigma}_h^1$ is the solution of (3), $\boldsymbol{\sigma}_h^2$ is the solution of (7), n_{dof}^1 and n_{dof}^2 are the respective sizes of the linear systems and n_t is the number of triangles. In table 2 the results for the regularized problem are displayed with the same notation.

Table 1. Results for cook's membrane

l	n_t	n^1_{dof}	n^2_{dof}	$\mathcal{J}_{ls}(\boldsymbol{\sigma}^1_h, \mathbf{u}^R_h)$	$\mathcal{J}_{ls}(\boldsymbol{\sigma}^2_h, \mathbf{u}^R_h)$	$\mathcal{J}_{ls}(\boldsymbol{\sigma}^1_h, \mathbf{u}^R_h)$	$\mathcal{J}_{ls}(\boldsymbol{\sigma}^2_h, \mathbf{u}^R_h)$
				$\lambda = 49999$	$\lambda = 49999$	$\lambda = 2$	$\lambda = 2$
0	44	717	1300	7.51712e-06	1.23805e-05	7.15095e-06	1.09624e-05
1	176	2885	5240	2.42195e-06	5.14683e-06	2.08703e-06	3.63318e-06
2	704	11577	21040	8.87635e-07	2.04684e-06	6.68831e-07	1.20104e-06
3	2816	46385	84320	3.60592e-07	8.23787e-07	2.32852e-07	4.11980e-07
4	11264	185697	337600	1.56550e-07	3.43616e-07	8.65879e-08	1.47983e-07
5	45056	743105	1351040	7.05565e-08	1.48839e-07	3.37006e-08	5.55008e-08
6	180224	2973057	5405440	3.24436e-08	6.64434e-08	1.35153e-08	2.15629e-08

Table 2. Results for the regularized problem

l	n_t	n^1_{dof}	n^2_{dof}	$\mathcal{J}_{ls}(\boldsymbol{\sigma}^1_h, \mathbf{u}^R_h)$	$\mathcal{J}_{ls}(\boldsymbol{\sigma}^2_h, \mathbf{u}^R_h)$	$\mathcal{J}_{ls}(\boldsymbol{\sigma}^1_h, \mathbf{u}^R_h)$	$\mathcal{J}_{ls}(\boldsymbol{\sigma}^2_h, \mathbf{u}^R_h)$
				$\lambda = 49999$	$\lambda = 49999$	$\lambda = 2$	$\lambda = 2$
0	49	816	1464	2.96362e-06	4.14240e-06	3.57976e-06	3.85810e-06
1	196	3248	5868	8.86412e-07	1.34541e-06	1.11751e-06	1.22544e-06
2	784	12963	23496	8.67680e-08	4.76183e-07	1.08365e-07	3.33871e-07
3	3136	51797	94032	7.66000e-09	1.64916e-07	9.41993e-09	9.13749e-08
4	12544	207081	376224	6.27767e-10	5.01953e-08	7.67974e-10	2.38911e-08
5	50176	828113	1505088	5.04845e-11	1.38663e-08	6.16212e-11	6.06266e-09
6	200704	3312033	6020736	4.11928e-12	3.63725e-09	5.02207e-12	1.52063e-09

Plotting the square root of the functional against the level of refinement yields the graphs in figure 2.

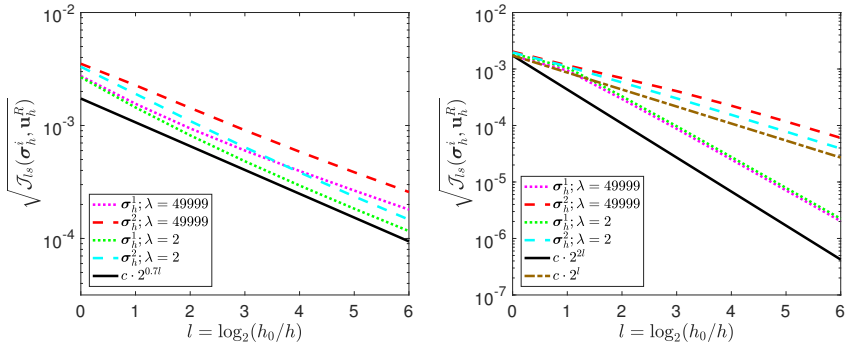

Fig. 2. Cook's membrane on the left and the regularized problem on the right

Our tests confirm the predicted convergence behaviour for the regularized problem. In case of the Cook's membrane problem both methods achieve only an order of convergence of approximately 0.7, which is due to the fact, that the solution of the continuous problem is less regular.

5 Postprocessing for Elementwise Symmetry on Average

Now we sketch a possible way for the construction of a modified stress approximation $\boldsymbol{\sigma}_h^S$ with the property that $\mathbf{as}\,\boldsymbol{\sigma}_h^S$ vanishes on average for all $T \in \mathcal{T}_h$. In order to keep the equilibration property (second equation in (3)) unaffected, we compute a correction in

$$\begin{aligned}\boldsymbol{\Sigma}_h^\perp &= \{\boldsymbol{\sigma}_h \in \boldsymbol{\Sigma}_h : \operatorname{div} \boldsymbol{\sigma}_h = \mathbf{0},\, \boldsymbol{\sigma}_h \cdot \mathbf{n} = \mathbf{0} \text{ on } \Gamma_N\} \\ &= \{\boldsymbol{\nabla}^\perp \boldsymbol{\chi}_h : \boldsymbol{\chi}_h \in H^1_{\Gamma_N}(\Omega)^2\,,\ \boldsymbol{\chi}_h|_T \in \mathcal{P}_2(T)^2\} =: \boldsymbol{\nabla}^\perp \boldsymbol{\Xi}_h\,,\end{aligned}$$

where $\boldsymbol{\Xi}_h$ is the standard conforming piecewise quadratic finite element space with zero boundary conditions on Γ_N. The constraint on the anti-symmetric part of the modified stress approximation $\boldsymbol{\sigma}_h^S = \boldsymbol{\sigma}_h + \boldsymbol{\nabla}^\perp \boldsymbol{\chi}_h$ then reads

$$0 = \left(\mathbf{as}\,\boldsymbol{\sigma}_h^S, \begin{bmatrix} 0 & 1 \\ -1 & 0 \end{bmatrix}\right)_{L^2(T)} = \left(\mathbf{as}\,\boldsymbol{\sigma}_h, \begin{bmatrix} 0 & 1 \\ -1 & 0 \end{bmatrix}\right)_{L^2(T)} - (\operatorname{div} \boldsymbol{\chi}_h, 1)_{L^2(T)}$$

for all $T \in \mathcal{T}_h$. A minimal correction $\boldsymbol{\chi}_h^\perp \in \boldsymbol{\Xi}_h$ is constructed such that

$$\begin{aligned}&\|\boldsymbol{\nabla}^\perp \boldsymbol{\chi}_h\|^2 \to \text{min! subject to the constraints} \\ &\qquad (\operatorname{div} \boldsymbol{\chi}_h, 1)_{L^2(T)} = \left(\mathbf{as}\,\boldsymbol{\sigma}_h, \begin{bmatrix} 0 & 1 \\ -1 & 0 \end{bmatrix}\right)_{L^2(T)} \text{ for all } T \in \mathcal{T}_h\end{aligned} \tag{9}$$

among all $\boldsymbol{\chi}_h \in \boldsymbol{\Xi}_h$. The inf-sup stability of the $\mathcal{P}_2 - \mathcal{P}_0$ element (in 2D) (cf. [4, Sect. 8.4.3]) and the coercivity in $H^1_{\Gamma_N}$ lead to the well-posedness of (9).

References

1. D. N. Arnold, F. Brezzi, and J. Douglas, *PEERS: A new mixed finite element for plane elasticity*, Japan J. Appl. Math. **1** (1984), 347–367.
2. D. N. Arnold, R. S. Falk, and R. Winther, *Finite element exterior calculus, homological techniques, and applications*, Acta Numerica **15** (2006), 1–155.
3. D. Boffi, F. Brezzi, and M. Fortin, *Reduced symmetry elements in linear elasticity*, Commun. Pure Appl. Anal. **8** (2009), 95–121.
4. D. Boffi, F. Brezzi, and M. Fortin, *Mixed finite element methods and applications*, Springer, Heidelberg, 2013.
5. Z. Cai and G. Starke, *Least squares methods for linear elasticity*, SIAM J. Numer. Anal. **42** (2004), 826–842.
6. A. Ern and M. Vohralík, *Polynomial-degree-robust a posteriori error estimates in a unified setting for conforming, nonconforming, discontinuous Galerkin, mixed discretizations*, SIAM J. Numer. Anal. **53** (2015), 1058–1081.
7. J. Gopalakrishnan and J. Guzmán, *Symmetric nonconforming mixed finite elements for linear elasticity*, SIAM J. Numer. Anal. **49** (2011), 1504–1520.
8. R. Stenberg, *Postprocessing schemes for some mixed finite elements*, Math. Model. Numer. Anal. **25** (1991), 151–167.